

# Liquid-Phase Synthesis of Flower-like and Flake-like Titanium Disulfide Nanostructures

Sujay Prabakar, Chris W. Bumby, and Richard D. Tilley\*

School of Chemical and Physical Sciences and Macdiarmid Institute of Advanced Materials and Nanotechnology, Victoria University of Wellington, New Zealand

Received January 13, 2009

Three-dimensional *flower-like* nanostructures of  $\text{TiS}_2$  and two-dimensional *flake-like* nanostructures of crystalline  $\text{TiS}_2$  have been synthesized using a facile solution method. On the basis of time-dependent experimental results, a growth mechanism has been proposed for these nanostructures. The injection temperature of the precursor plays a key role in the formation of the *flower-like* and *flake-like* morphology. The nanostructures have been characterized by X-ray powder diffraction, scanning electron microscopy, and transmission electron microscopy. The surface area of the nanostructures is also reported.

## Introduction

Metal chalcogenide materials with layered structures such as  $\text{TiS}_2$ ,  $\text{NbS}_2$ ,  $\text{MoS}_2$ ,  $\text{WS}_2$ , and  $\text{SnS}_2$  have attracted considerable interest in recent years because of their electronic properties and potential applications.<sup>1–4</sup>  $\text{TiS}_2$  and its intercalation compounds have been studied intensively and shown to be promising cathode materials in rechargeable batteries<sup>5</sup> and as potential hydrogen storage materials.<sup>6</sup>

$\text{TiS}_2$ , like the rest of the group IVA dichalcogenides, crystallizes in the hexagonal  $\text{CdI}_2$  structure, a layered compound with repeating subunits, made by a layer of Ti atoms and two layers of S atoms.<sup>7</sup> There is strong bonding between atoms in the Ti and S layers, whereas weak van der Waals forces dominate the bonding between the S and S layers.

Various morphologies of  $\text{TiS}_2$  such as nanotubes,<sup>5</sup> nanoclusters,<sup>8</sup> fullerenes,<sup>9</sup> nanodisks,<sup>10</sup> whiskers,<sup>11</sup> and thin films<sup>12</sup> have been successfully synthesized. With respect to the synthesis of three-dimensional (3D) nanostructures, morphologies such as *flower-like* patterns and dendritic crystals of  $\text{TiS}_2$  have been synthesized, by a chemical vapor transport

approach.<sup>13,14</sup> However, the controlled wet chemical synthesis of *flower-like* nanostructures of  $\text{TiS}_2$  has not previously been achieved.

Reports have been observed for the synthesis of *flake-like* nanostructures for materials such as  $\text{SnS}_2$  and  $\text{MoS}_2$ , their growth attributed to their crystal structure.<sup>15,16</sup> To our knowledge, the synthesis of *flake-like* nanostructures in  $\text{TiS}_2$  is yet to be achieved.

Moreover, the facile control of whether materials adopt two-dimensional (2D) structures such as nanoflakes or nanoplatelets and 3D structures such as nanoflowers or nanorods is still difficult and requires complex synthetic techniques.<sup>13,14</sup> However, a colloidal synthesis offers a more promising approach with advantages of being low cost in preparation and suitable for large-scale production.

In this paper we report a simple one-step solution phase route to synthesize elegant 3D *flower-like* nanostructures of  $\text{TiS}_2$  and 2D *flake-like* nanostructures. This is the first report of the synthesis of *flake-like* nanostructures and synthesis in solution of *flower-like* nanostructures of  $\text{TiS}_2$ . These nanostructures were obtained from the reaction of titanium tetrachloride with elemental sulfur in the noncoordinating solvent 1-octadecene. It was found that changing the injection temperature could easily control whether a 2D or 3D morphology of nanostructures was obtained. On the basis of the evolution of the structure and morphology with reaction time, a growth mechanism of the *flower-like* and *flake-like* nanostructures has been elucidated.

## Experimental Section

All of the chemicals used in this experiment were of analytical grade. In a typical synthesis, 0.192 g (6.00 mmol) of sulfur was

- (1) Tenne, R.; Margulis, L.; Genut, M.; Hodes, G. *Nature* **1992**, *360*, 444.
- (2) Feldman, Y.; Wasserman, E.; Srolovitz, D. J.; Tenne, R. *Science* **1995**, *267*, 222.
- (3) Nath, M.; Rao, C. N. R. *Angew. Chem., Int. Ed.* **2002**, *41*, 18.
- (4) Hong, S. Y.; Popovitz-Biro, R.; Prior, Y.; Tenne, R. *J. Am. Chem. Soc.* **2003**, *125*, 10470.
- (5) Tao, Z.-L.; Xu, L.-N.; Gou, X.-L.; Chen, J.; Yuan, H.-T. *Chem. Commun.* **2004**, 2080.
- (6) Chen, J.; Li, S.-L.; Tao, Z.-L.; Shen, Y.-T.; Cui, C.-X. *J. Am. Chem. Soc.* **2003**, *125*, 5284.
- (7) Wilson, J. A.; Yoffe, A. D. *Adv. Phys.* **1969**, *18*, 193.
- (8) Mainwaring, D. E.; Let, A. L.; Murugaraj, P. *Solid State Commun.* **2006**, *140*, 355.
- (9) Margolin, A.; Popovitz-Biro, R.; Albu-Yaron, A.; Rapoport, L.; Tenne, R. *Chem. Phys. Lett.* **2005**, *411*, 162.
- (10) Park, K. H.; Choi, J.; Kim, H. J.; Oh, D.-H.; Ahn, J. R.; Son, S. *Small* **2008**, *7*, 945.
- (11) Zhang, Y.; Li, Z.; Jia, H.; Luo, X.; Xu, J.; Zhang, X.; Yu, D. *J. Cryst. Growth* **2006**, *293*, 124.
- (12) Let, A. L.; Mainwaring, D. E.; Rix, C. J.; Murugaraj, P. *J. Phys. Chem. Solid* **2007**, *68*, 1428.

- (13) Tao, Y.-R.; Wu, X.-C.; Zhang, Y.-L.; Dong, L.; Zhu, J.-J.; Hu, Z. *Cryst. Growth Des.* **2008**, *8* (8), 2990.
- (14) Ma, J.; Jin, H.; Liu, X.; Fleet, M. E.; Li, J.; Cao, X.; Feng, S. *Cryst. Growth Des.* **2008**, *8* (12), 4460.
- (15) Yang, Q.; Tang, K.; Wang, C.; Zhang, D.; Qian, Y. *J. Solid State Chem.* **2002**, *164*, 106.
- (16) David, J. S.; Pradeep, T.; Joydeep, B.; Umesh, W. V. *J. Am. Soc. Mass Spectrom.* **2007**, *18*, 2191.

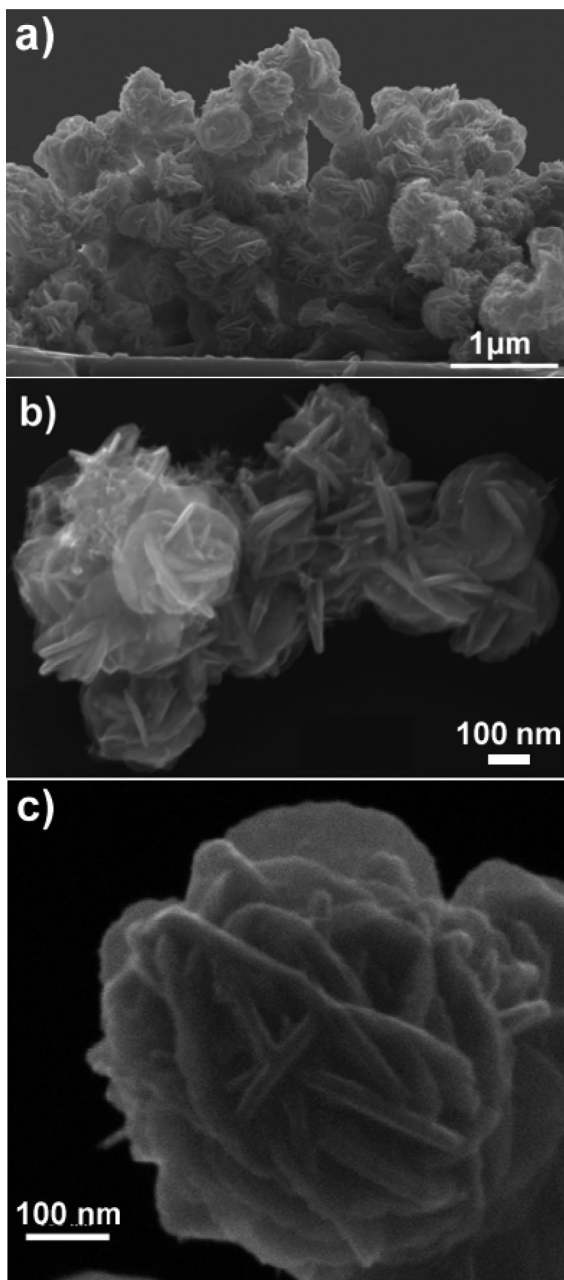


**Figure 1.** SEM images (a) and (b) are low-magnification images of flower-like  $\text{TiS}_2$  nanostructures and (c) individual flower-like nanostructures.

dissolved in 20 mL of 1-octadecene (90%, Aldrich) and gradually heated to 300  $^{\circ}\text{C}$  and degassed for 30 min. Titanium tetrachloride (0.10 mL, 1.00 mmol) ( $\text{TiCl}_4$  98.5%, Aldrich) was injected swiftly into the stirring sulfur solution and the mixture turned black instantly. The solution was allowed to react for 10 min and then allowed to cool to room temperature. A black powder containing flower-like  $\text{TiS}_2$  nanostructures was obtained. In a second reaction, titanium tetrachloride was injected at a temperature of 150  $^{\circ}\text{C}$  and then over 15 min the reaction temperature was increased to 300  $^{\circ}\text{C}$  and then allowed to react for 10 min. The reaction proceeded in a similar fashion with a rapid change in color followed by the formation of a black precipitate. The morphologies of the final product were observed to be flake-like. All experiments were conducted in a  $\text{N}_2$  atmosphere, and the black solids obtained from both the reactions were collected by centrifugation and purified by washing with toluene and methanol repeatedly.

The resulting products were analyzed by scanning electron microscopy (SEM) on a JSM-6500F microscope. Transmission

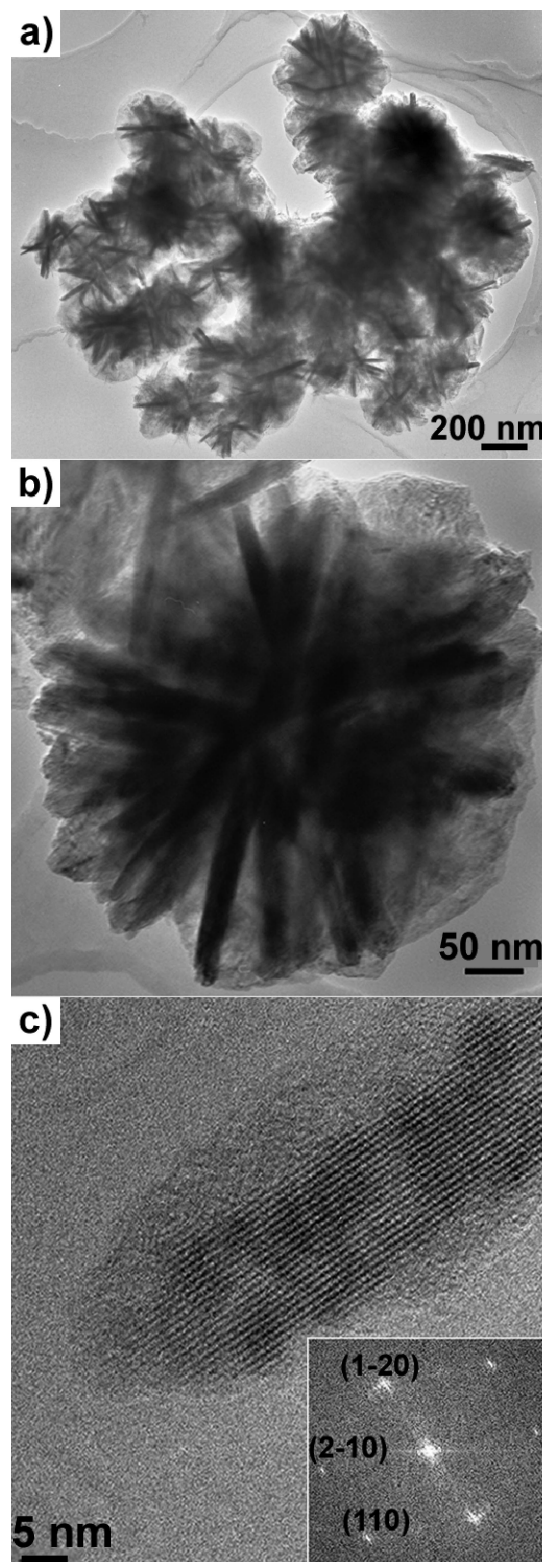


**Figure 2.** (a) Low-resolution TEM image of as-prepared  $\text{TiS}_2$  nanoflowers; (b) a single nanoflower exhibiting rodlike growth originating from the center of the flake; (c) high-resolution TEM image of a nanopetal and (inset) FFT pattern of the corresponding image.

electron microscopy images (TEM) images and electron diffraction patterns were obtained using a JEOL 2010 transmission electron microscope operating at 200 keV equipped with a double tilt sample holder. Specimens for TEM investigations were sonicated in hexane and a drop of the solution was placed on a carbon-film-coated holey copper grid. The Brunauer–Emmett–Teller (BET) measurements

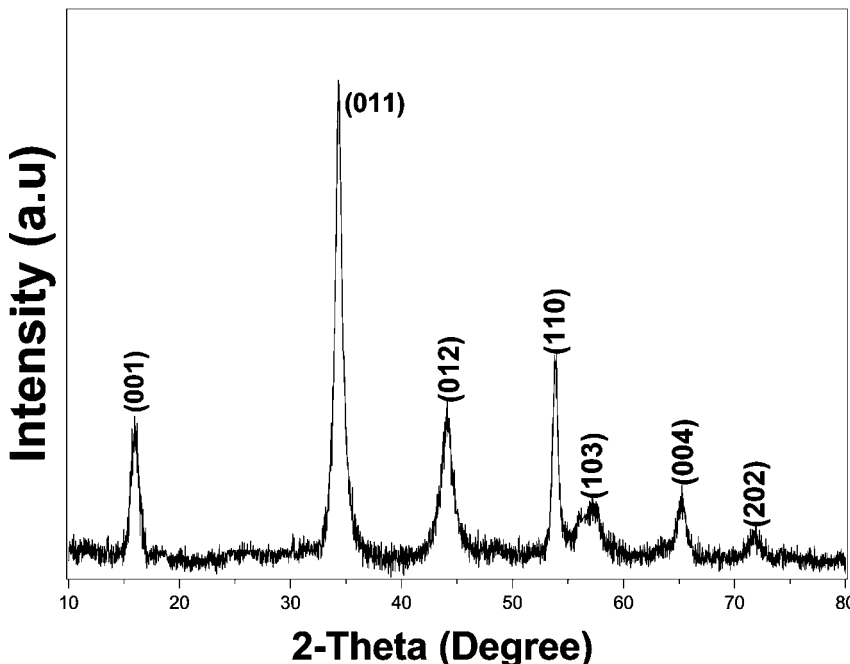


**Figure 3.** XRD pattern of the  $\text{TiS}_2$  flower-like nanostructure.

were determined with a Micromeritics ASAP 2010 Accelerated Surface Area and Porosimetry System. Powder X-ray diffraction patterns were acquired on a Phillips PW 1720 X-ray generator using Cu K $\alpha$  radiation.

## Results and Discussion

The first reaction had both an injection and a reaction temperature of 300 °C of the titanium tetrachloride in the elemental sulfur solution. Low- and medium-magnification SEM images of the nanostructured materials formed are shown in Figure 1a,b.

From the images it may be observed that the structures are three-dimensional, partially spherical, and flower-like in appearance. Figure 1a is a typical SEM image and shows the flower-like nanostructures aggregated together. The flower-like nanostructures tend to cluster in groups of around 10–50. Individual flower-like nanostructures are typically between 100 and 500 nm in size. Higher magnification images showing more detailed morphology of the flower-like nanostructures are shown in Figure 1b,c and indicate that the flower-like nanostructures are built from tens of nanopetals. As can be seen in Figure 1c, individual flowers are made of randomly aligned nanopetals of about 100–500 nm in length and 20–50 nm in width. Sonication of the nanostructures did not break them into discrete petals, suggesting that the nanostructures are integrated and not an aggregation of nanopetals.

Further insight into the morphology and structure of the flower-like nanostructures was gained using low- and high-resolution transmission electron microscopy (TEM). The TEM images in parts (a) and (b) of Figure 2 show aggregates of flower-like nanostructures and an individual flower-like nanostructure, respectively. From the images it may be seen that the petals are about 25 nm in width and taper toward the edge. The nanopetals are crystalline and the TEM image

in Figure 2c shows clearly observable lattice fringes. Fast Fourier transform (FFT) analysis (inset) of the corresponding image matched the crystal structure of titanium disulfide viewed down the [001] orientation.

An X-ray powder diffraction pattern of the  $\text{TiS}_2$  flower-like nanostructure is shown in Figure 3. The reflections could be readily indexed to the hexagonal phase of  $\text{TiS}_2$ .<sup>17</sup>

**Variation of Reaction Time and Growth Mechanism.** To investigate the growth mechanism of the flower-like  $\text{TiS}_2$ , experiments were performed at 300 °C where small aliquots were removed from the reaction flask at times of 30, 60, and 90 s and quenched in an ice bath. The SEM images shown in Figure 4 are of the samples obtained at these different reaction times and illustrate the evolution of the morphology of the  $\text{TiS}_2$  flower-like nanostructure. The sample taken after a 30 s reaction time is shown in the image Figure 4a. The products consist of a spherical core of size 200–300 nm with blisters growing from this core. We define these structures as *spheres with surface blisters*. The surface blisters are roughly semispherical in shape with diameters typically less than 35 nm. Energy-dispersive X-ray (EDX) analysis in both SEM and TEM of the spheres with surface blisters showed that their composition was  $\text{TiS}_{1.3}\text{Cl}_{0.8}$ .

An SEM image of a typical particle from the sample with a reaction time of 60 s is shown in Figure 4b. From SEM analysis it was found that over 80% of the product were particles similar to the one shown in Figure 4b, which we call *spheres with protuberances* and 20% of the product still remained as spheres with surface blisters. As shown in Figure 4b, a typical sphere with protuberances has a spherical core of similar size and structure to the spheres with surface blisters. As can be seen in Figure 4b, the protuberances are made of platelets that are randomly oriented, growing off the spherical core. From high-resolution TEM it was

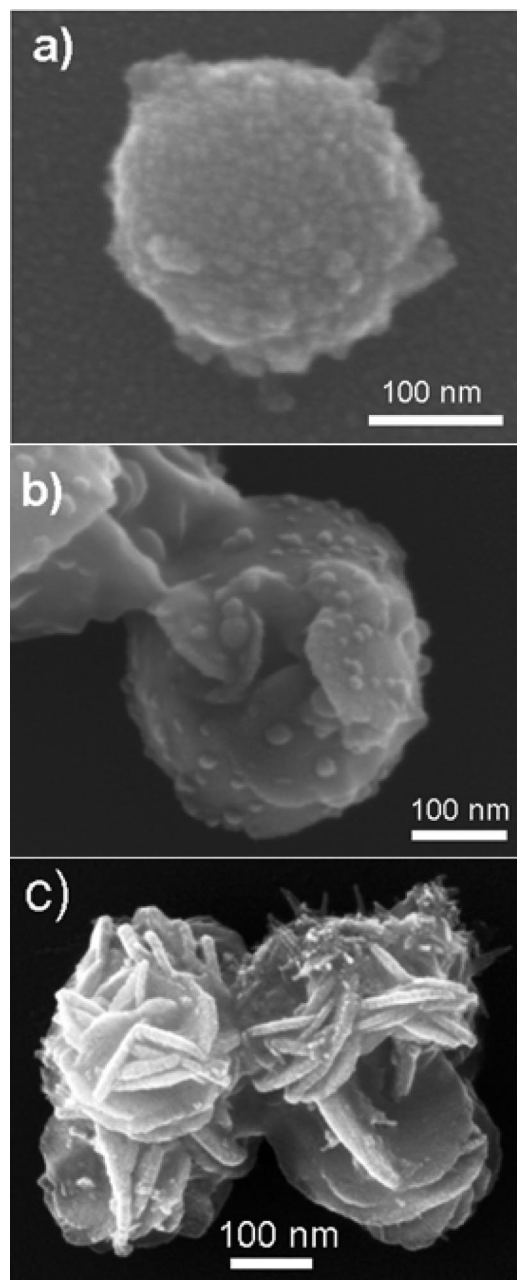


**Figure 4.** SEM images of the products obtained at different growth stages: (a) 30 s, (b) 60 s, and (c) 90 s.

discovered that they are 10–100 atomic layers in thickness and typically 35–250 nm horizontally. TEM studies on both surface blisters and protuberances showed that they were crystalline and were composed of stoichiometric  $\text{TiS}_2$ . However, from selected area electron diffraction (SAED), the spherical core was found to be amorphous.

At 90 s, the sample contained flower-like nanostructures of  $\text{TiS}_2$  in a 100% yield. A typical flower-like nanostructure is shown in Figure 4c. As can be seen from Figure 4c, these structures are made of randomly aligned nanopetals originating from the center that are so large that the spherical core is no longer evident. SAED indicated that the flower-like nanostructures were highly crystalline. Reactions for longer time periods were also found to form identical flower-like nanostructures, suggesting that they are the final

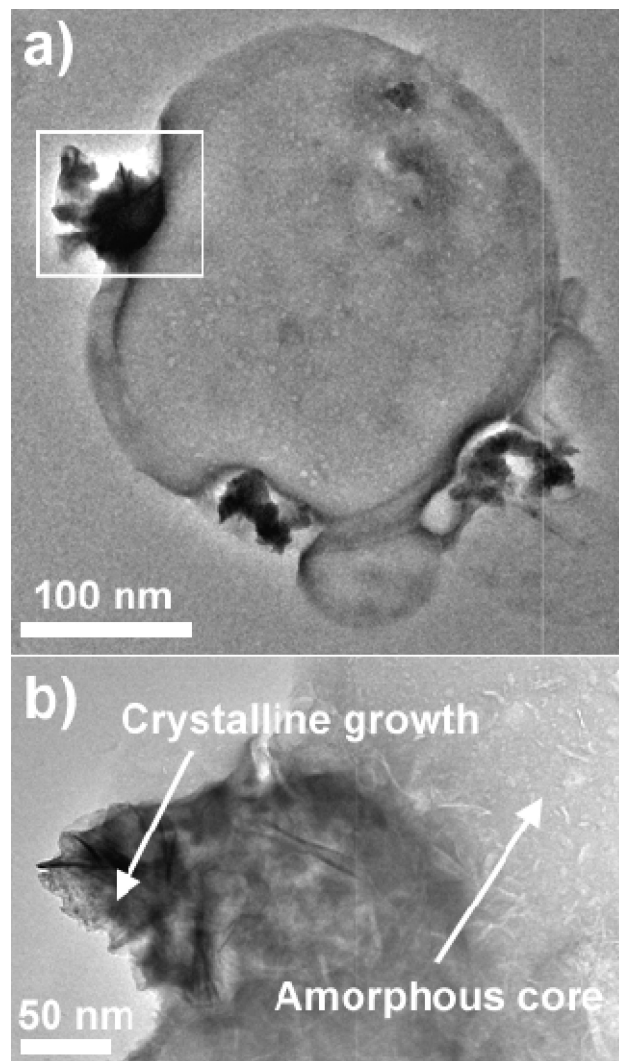
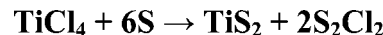


**Figure 5.** (a) Low-magnification TEM image of a sphere isolated at 60 s. (b) Higher magnification image of the rectangular section in Figure 5a, indicating the crystalline and amorphous part of the sphere.

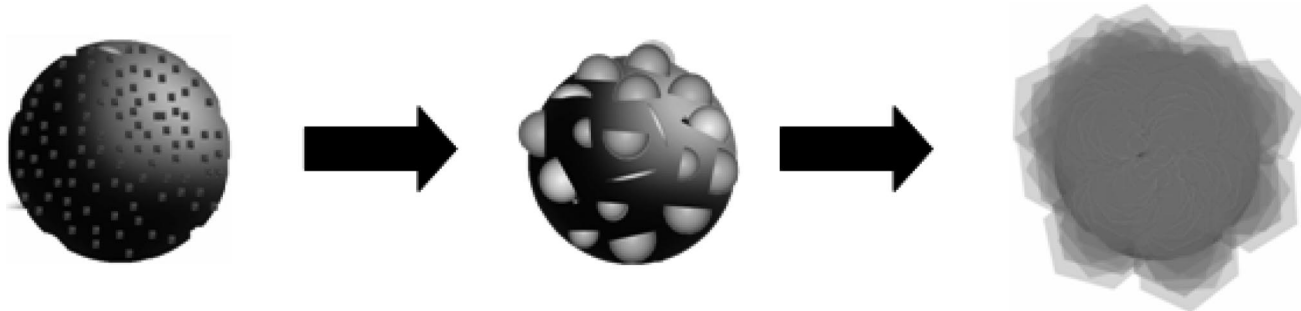
**Scheme 1. Reaction for the Synthesis of  $\text{TiS}_2$  Flower-like Nanostructures**



thermodynamic product. EDX analysis in SEM and TEM of the final flower-like nanostructures indicated a composition of  $\text{TiS}_{1.8}$ .

TEM analysis of the spheres with surface blisters was undertaken to further characterize the intermediate structure. The TEM image of a typical sphere with surface blisters isolated at 60 s is shown in Figure 5a and a higher magnification image in Figure 5b. SAED of the area boxed in white containing the surface blister indicated that the surface blister was crystalline and SAED of the spherical core gave an amorphous diffraction pattern.

**Chemical Reaction.** The formation of crystalline  $\text{TiS}_2$  from  $\text{TiCl}_4$  and elemental sulfur most likely occurs through the overall reaction shown in Scheme 1. Sulfur has been known to act as both the reductant and sulfiding agent at high temperatures.<sup>18–21</sup> The  $\text{TiS}_{1.3}\text{Cl}_{0.8}$  stoichiometry of the spheres

Scheme 2. Growth Mechanism of the  $\text{TiS}_2$  Flower-like Nanostructures

with surface blisters indicates that a reaction may also occur to form amorphous  $\text{TiS}_x\text{Cl}_y$  compounds.

**Growth Mechanism.** On the basis of the electron microscopy results shown in Figures 4 and 5, the growth mechanism for the formation of the flower-like nanostructures was elucidated and is depicted schematically in Scheme 2.

During the initial stages of nucleation, amorphous spheres between 200 and 300 nm with an approximate composition of  $\text{TiS}_{1.3}\text{Cl}_{0.8}$  form. These spheres have small crystalline blisters of  $\text{TiS}_2$  on the surface to give spheres with surface blisters. As the reaction continues, the inner amorphous spherical core remains constant in size and the growth occurs on the surface of the spheres as the surface blisters grow into bigger protuberances. As the reaction continues to 90 s, these protuberances have continued to grow in size to become full crystalline flower-like petals. These observations agree with previous reports of growth mechanisms involving a multistage growth process.<sup>22–25</sup>

Thus, the growth and morphology of the flower-like nanostructures may be understood as follows. The initial particles formed are amorphous and thus adopt a spherical shape. The surface of the spheres act as nucleation sites for the formation of small crystalline blisters of  $\text{TiS}_2$ . As the reaction proceeds, it is energetically more favorable for the crystalline  $\text{TiS}_2$  blisters to grow, which they do via protuberances into full crystalline flower-like petals with the blisters on the surface of these spheres providing high-energy sites for crystalline growth.<sup>26,27</sup> The platelike 2D shape of the protuberances and flower-like petals originates from the layered structure of  $\text{TiS}_2$ , which grows preferentially along the *a*- and *b*-axes compared to the *c*-axis.

**Flake-like Nanostructures.** In a second reaction the injection temperature of the titanium source into the elemental sulfur was decreased to 150 °C. After injection at 150 °C, the temperature of the solution was gradually increased to 300 °C over a period of 15 min and the reaction further heated for 10 min. The as-synthesized product was purified and dispersed in hexane for analysis by SEM and TEM. SEM

and TEM images of the products are shown in Figure 6. As can be seen from Figure 6a, the product was highly irregularly shaped  $\text{TiS}_2$  fragments, which we refer to as  $\text{TiS}_2$  flake-like nanostructures that were typically tens of micrometers in size. The higher magnification SEM image shown in Figure 6b shows that each of these flake-like nanostructures were made of smaller flakes about a micrometer in size attached to each other in random orientations to form discrete flake-like nanostructures and do not disintegrate upon sonication. Figure 6c is a representative TEM image in which Figure 6c shows an individual flake-like nanostructure of  $\text{TiS}_2$ , showing good agreement with SEM images, and illustrates that the nanostructures are made of flaky protrusions. The light contrast in many areas of the TEM image in Figure 6c indicates the thin 2D nature of the flake-like nanostructures. The flake-like nanostructures were found to be crystalline and SAED patterns could be indexed to the hexagonal phase of  $\text{TiS}_2$ . EDX analysis was carried out on individual flakes of  $\text{TiS}_2$ , which showed good agreement with 1:2 molar ratios of titanium to sulfur.

**Growth Mechanism.** To understand the formation of the flake-like nanostructures, the reaction was repeated with small aliquots removed at different reaction times in a fashion similar to the method used for the flower-like nanostructures. The product in all the aliquots removed were analyzed by SEM and TEM and even those taken after only 1 s were flake-like nanostructures with the same size and morphology of those found at the longer reaction times and shown in Figure 6. These results show that the flake-like nanostructures are formed immediately after injection and prevented the isolation of initial products.

The formation of 2D flake-like nanostructures in dichalcogenide systems originates from the layered crystal structure. Flake-like nanostructures form with growth along the [100] and [010] directions, these directions being more favorable because of stronger bonding than that seen from growth in the longer [001] direction.<sup>28</sup>

**Morphological Control.** The results show that the final morphology of the  $\text{TiS}_2$  nanostructure can be controlled by the nature of the initial nuclei. At a lower injection temperature of 150 °C flake-like nanostructures are obtained, most likely from the instant nucleation of  $\text{TiS}_2$  flakes. At a higher injection temperature of 300 °C, flower-like nanostructures are obtained through the formation of spherical nuclei of  $\text{TiS}_x\text{Cl}_y$ . This understanding of the controlled and

- (19) Li, X. L.; Li, Y.-D. *Chem. Eur. J.* **2003**, *9*, 2726.
- (20) Ge, J. P.; Li, Y.-D. *Chem. Commun.* **2003**, *19*, 2498.
- (21) Ge, J. P.; Li, Y.-D. *Adv. Funct. Mater.* **2004**, *14*, 157.
- (22) Burda, C.; Chen, X. B.; Narayanan, R.; El-Sayed, M. A. *Chem. Rev.* **2005**, *105*, 1025.
- (23) Cheng, Y.; Wang, Y. S.; Zheng, Y. H.; Qin, Y. *J. Phys. Chem. B* **2005**, *109*, 11548.
- (24) Penn, R. L. *J. Phys. Chem. B* **2004**, *108*, 12707.
- (25) Park, J.; Privman, V.; Matijevic, E. *J. Phys. Chem. B* **2001**, *105*, 11630.
- (26) Chang, Y.; Teo, J. J.; Zeng, H. C. *Langmuir* **2005**, *21*, 1074.
- (27) Xi, G.; Xiong, K.; Zhao, Q.; Zhang, H.; Qian, Y. *Cryst. Growth Des.* **2006**, *6*, 577.

- (28) Wells, A. F. *Structural Inorganic Chemistry*, 5th ed; Oxford University Press: London, 1984.

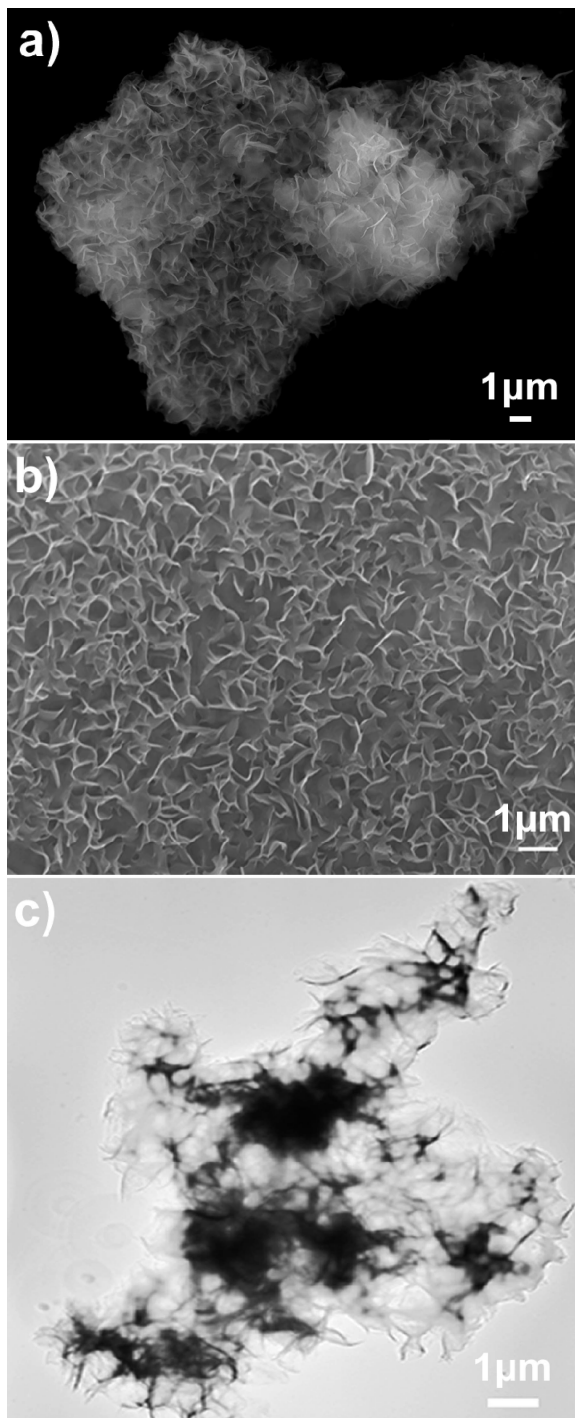


**Figure 6.** (a) Low-resolution SEM image of the flake-like nanostructures; (b) higher magnification view of the flakes; (c) TEM image of a single  $\text{TiS}_2$  flake.

selected growth of both flower-like and flake-like nanostructures is highly significant for understanding the growth of all materials with similar layered structures including industrially important  $\text{MoS}_2$ ,  $\text{NbS}_2$ , and  $\text{WS}_2$ .

**BET Surface Area Measurements.**  $\text{TiS}_2$  is known to have possible applications as hydrogenation catalysts and hydrogen storage devices. For these applications high surface area is important. Hence, surface area measurements were conducted on both flower-like and flake-like nanostructures and were found to be  $32 \text{ m}^2 \text{ g}^{-1}$  and  $19 \text{ m}^2 \text{ g}^{-1}$ , respectively (Figure 7). The surface area of our flower-like nanostructures were found to

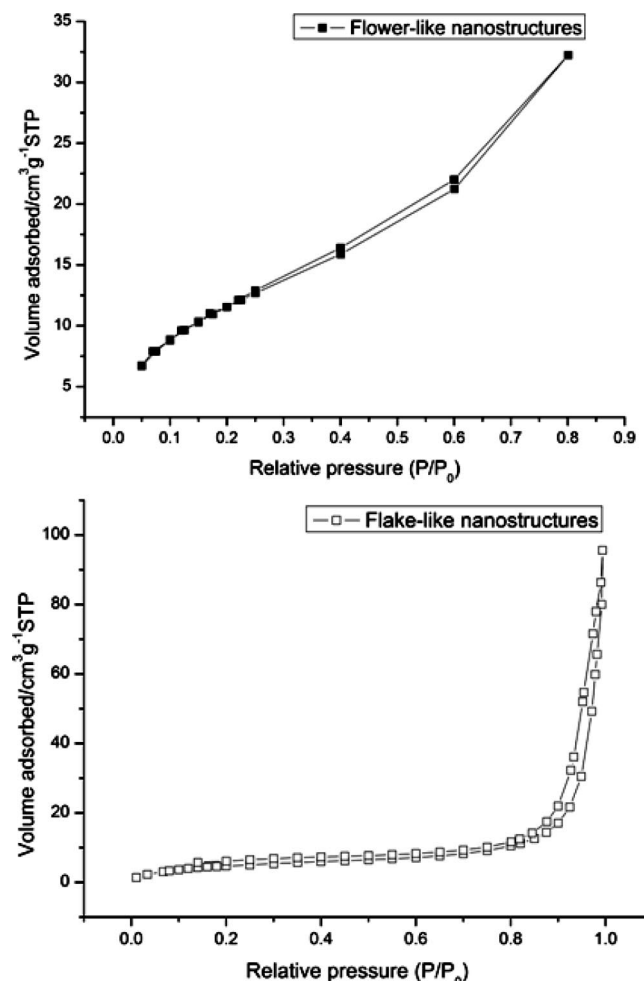


**Figure 7.** BET (isothermal adsorption/desorption plot) surface area measurements of  $\text{TiS}_2$  nanostructures.

be more than that reported for  $\text{TiS}_2$  nanotubes by Chen et al.<sup>29</sup> This high surface area indicates that these materials should have excellent performance as catalyst carriers and hydrogen storage devices.

## Conclusion

In summary, elegant flower-like and flake-like nanostructures of  $\text{TiS}_2$  were, for the first time, synthesized by a colloidal route. The morphology and chemical composition of the as-synthesized nanostructures are characterized, and a possible growth mechanism for the formation of these nanostructures has been elucidated. The key factors in controlling the morphologies were discussed based on a clear understanding of the growth mechanism. The surface area of flower-like and flake-like  $\text{TiS}_2$  nanostructures have also been reported. The synthetic route is expected to be applicable in the synthesis of other metal dichalcogenide layered systems.

**Acknowledgment.** R.D.T. thanks the MacDiarmid Institute for funding. S.P., C.B., and R.D.T. thank FRST for funding through Grant IIOF VICX0601.

CM900110H